

## Research Article

# Water-Soluble and Biodegradable Pectin-Grafted Polyacrylamide and Pectin-Grafted Polyacrylic Acid: Electrochemical Investigation of Corrosion-Inhibition Behaviour on Mild Steel in 3.5% NaCl Media

**R. Geethanjali, A. Ali Fathima Sabirneeza, and S. Subhashini**

*Department of Chemistry, Avinashilingam Institute for Home Science and Higher Education for Women, Coimbatore 641043, India*

Correspondence should be addressed to S. Subhashini; [subhashini\\_adu@yahoo.com](mailto:subhashini_adu@yahoo.com)

Received 16 October 2013; Accepted 21 November 2013; Published 7 April 2014

Academic Editors: J. M. Deitzel, K. Dhara, M. Lavorgna, P. B. Wagh, and H. S. Yathirajan

Copyright © 2014 R. Geethanjali et al. This is an open access article distributed under the Creative Commons Attribution License, which permits unrestricted use, distribution, and reproduction in any medium, provided the original work is properly cited.

Pectin-g-polyacrylamide (denoted as Pec-g-PAAm) and pectin-g-polyacrylic acid (denoted as Pec-g-PAA) were synthesized using pectin, acrylamide, and acrylic acid as starting materials. The grafted polymers were characterized using Fourier transform infrared spectroscopy (FTIR), thermogravimetric analyser (TGA), and scanning electron microscopy (SEM). The corrosion inhibition behaviour of the grafted polymers on mild steel in 3.5% NaCl was evaluated electrochemically through Tafel polarization and impedance studies. The corrosion inhibition performance of both the polymers was found to be around 85%.

## 1. Introduction

The importance of mild steel is well known owing to its cost, process-ability, and weld-ability when used for infrastructures in marine environments like ship hulls, oil rings, off-shore platforms, coastal facilities and sheet piling, and so forth. The mild steel is preferred over stainless steel in chloride environments, because the cost of stainless steel good enough to resist corrosion is far too great. There are several advantages in selecting the mild steel, but it still suffers uniform or generalised corrosion, which is of considerable economic importance.

The corrosion inhibition mechanism involves strong adsorption of inhibitor molecules on the active sites of metal and thereby preventing cathodic and anodic reactions of the metal. Polymers are selected for corrosion inhibition because of the superior performance when compared with their monomer analogues in active adsorbing on the corrosive sites of the metal [1]. The improved performances of the polymeric materials are ascribed to their multiple adsorption sites for bonding with the metal surface. The polymer provides two advantages: a single polymeric chain displaces many water molecules from the metal surface, thus making the process

entropically favourable and the presence of multiple bonding sites makes the desorption of the polymers a slower process [2].

Research activities in recent times are geared towards revealing green corrosion inhibitors to replace the toxic inorganic and organic compounds. Naturally occurring substances have been found to readily satisfy this need. Apart from being readily available, cheap, and a renewable source of materials, naturally occurring substances are eco-friendly and ecologically acceptable [3].

Xu et al. [4] synthesized polyaspartic acid-melamine (PASPM) grafted copolymer and evaluated its  $\text{CaCO}_3$  and  $\text{Ca}_3(\text{PO}_4)_2$  scale inhibition performance and dispersion capacity for ferric oxide. The PASPM copolymer efficiently inhibited  $\text{CaCO}_3$  scale and possessed good dispersion capacity for  $\text{Fe}_2\text{O}_3$ , both the performances being highly dependent on dosage. The author explains that this could be because of N-containing triazine heterocyclic ring of PASPM copolymer which could chelate  $\text{Ca}^{2+}$  to form stabilized and dissoluble chelates, thereby increasing the solubility of calcium salts in water. Ren et al. [5] synthesized lignin terpolymer by graft copolymerization of both dimethyl diallyl ammonium chloride (DMDAAC) and acrylamide (AM) onto lignin which

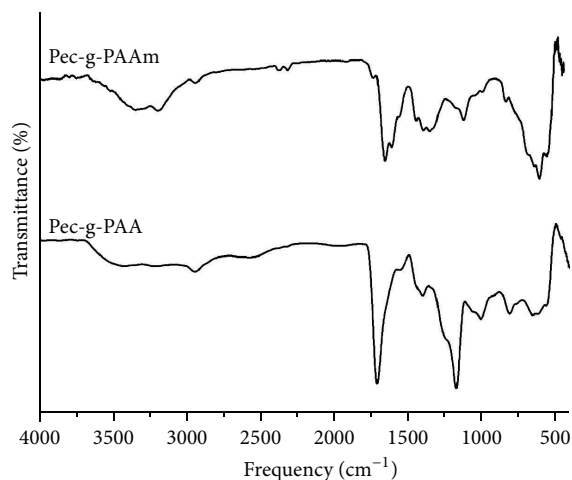


FIGURE 1: FTIR spectrum of Pec-g-PAAm and Pec-g-PAA.

provided a highest corrosion inhibition percentage of 95% in 10% HCl acid medium at 25°C and 80°C. The corrosion inhibition performance may be due to the comprehensive synergistic effect through the graft reaction among lignin, AM, and DMDAAC.

Fares et al. [6] studied the corrosion inhibition performance of pectin as promising green corrosion inhibitor of aluminium in hydrochloric acid solution. Polyacrylamide was grafted on okra fruit mucilage and corrosion behaviour was investigated in acid medium [7]. Akbarzadeh et al. [8] evaluated corrosion inhibition of mild steel in near neutral solution by kraft and soda lignins extracted from oil palm empty fruit bunch.

Several polymers have been grafted onto the backbone of natural polymers like starch, chitosan, alginate, pectin, carrageenan, and so forth and used as hydrogels in drug-delivery systems, sensor applications, flocculating agents and adsorbents, and so forth.

In this paper, the natural polymer pectin was modified by grafting it with polyacrylic acid (Pec-g-PAA) and polyacrylamide (Pec-g-PAAm), and the compatibility as corrosion inhibitors has been evaluated for mild steel in neutral medium, and the optimum ratio has been found in the study. Pectin is known to be rapidly degraded by colonic microorganisms which makes it a potential carrier for colon targeted drug delivery. Pec-g-PAA and Pec-g-PAAm were reported as pH sensitive hydrogels to be used in the colon drug delivery [9–12]. Hence the polymers can be claimed to be biodegradable and environmentally friendly.

Though weight-loss measurement is a reliable and universally accepted method, the huge time factor for studying the mild steel corrosion in sodium chloride medium has to be considered. Therefore, electrochemical measurements could be the best alternative for testing corrosion at a faster rate with more information and can be used in field detection combined with other methods. After all, electrochemical technique is a nondestructive, quantitative technique and a powerful tool for researching corrosion process [13].

## 2. Experimental

**2.1. Instruments and Chemicals.** Instruments used in the present research include Remi-Magnetic stirrer, Shimadzu Electronic weighing balance, Tensor-27 FTIR spectrometer, Christ Freeze dryer, Extar SII TG/DTA6300 Thermo gravimetric analyser and FESEM Quanta-250 scanning electron Microscope, and Biologic SP-150 Frequency Response Analyser.

The chemicals used in the present invention include pectin (SD fine), acrylamide (Himedia), acrylic acid (Himedia), acetone (SD fine), sodium hydroxide (Merck), potassium persulphate (Merck), and sodium bisulphite (Merck).

**2.2. Water-Soluble Pec-g-PAAm and Pec-g-PAA.** The graft polymerization of acrylamide on pectin was carried out by slightly modifying the procedure given by Mishra et al. [10] to achieve water soluble products as per our requirement. Mishra et al. synthesized a pH sensitive hydrogel using the pectin and acrylamide, but in this study, the solubility of the polymer products was achieved by adding sodium hydroxide to the reaction mixture and carrying out the polymerization in acetone/water medium. When pectin was present in higher amount, insoluble hydrogels resulted, so the amount of the pectin was taken in minimum quantities. The detailed reaction procedure is as follows.

1.9 g of recrystallized acrylamide and 0.1 g of pectin were as mixed in 5 g of water and 2.5 g of acetone. The reaction mixture was neutralised with 0.2 mL of 30% sodium hydroxide. Then 0.2 mL of 10% polyvinyl alcohol was added. The whole reaction mixture was purged with nitrogen for 30 minutes to ensure an inert atmosphere. As a redox initiator 0.1 mL of potassium persulphate/0.05 mL of sodium bisulphite was added, and the reaction was allowed to continue for 4 hours. The reaction temperature was maintained in the range of 45–50°C. The resulting viscous solution was precipitated using acetone. The fibrous polymer products were lyophilized and used for further studies. The same procedure was followed for graft polymerization of acrylic acid on pectin.

### 2.3. Characterization of the Polymers

**2.3.1. FTIR Spectroscopy.** The structures of the prepared polymers were confirmed using FTIR spectrometer having an ATR assembly. The scan range was 400–4000 cm<sup>-1</sup>.

**2.3.2. Thermogravimetric Analysis.** The thermal stability of the polymers was determined using thermogravimetric analyser at a heating rate of 20°C/minute from 30 to 650°C under Nitrogen purge.

**2.3.3. Scanning Electron Microscopic and Elemental Analysis.** The grafted polymers were dissolved in water and coated as a thin layer on carbon tape and imaged in a SEM instrument.

**2.4. Electrochemical Measurements.** The specimen used for the study is mild steel coupon of 1 cm<sup>2</sup> exposed surface area attached to a steel rod by brass welding. Before each test the specimen was ground using different grades of

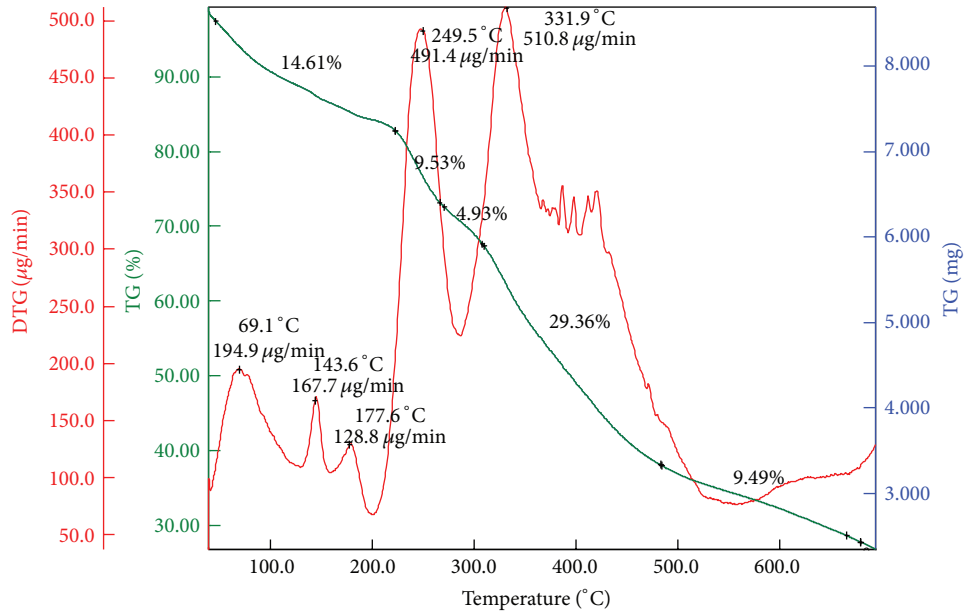


FIGURE 2

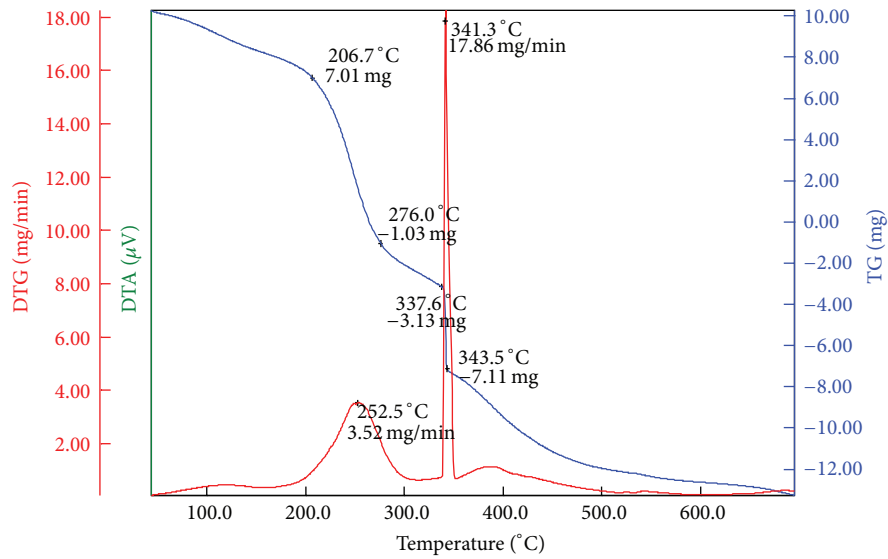


FIGURE 3

emery paper to achieve a mirror-finish polished surface. A platinum electrode as counter electrode and a calomel electrode containing saturated potassium chloride solution as reference electrode were used for the electrochemical studies in 3.5% sodium chloride as electrolyte solution. The electrochemical investigation was conducted as two different phases, namely potentiodynamic polarization and electrochemical impedance measurements.

The potentiodynamic polarization was conducted with constant sweep rate of 1 mV/sec in the range of -0.1 to -1 mV with respect to  $E_{corr}$ .

Various corrosion kinetic parameters such as corrosion current density ( $I_{corr}$ ), corrosion potential ( $E_{corr}$ ), and anodic

and cathodic Tafel slopes ( $b_a$  and  $b_c$ ) were obtained. Corrosion current density was measured from the intersection point obtained by the extrapolation of Tafel lines. The inhibition efficiency can be calculated from corrosion current  $I_{corr}$  using the following equation:

$$IE (\%) = 100 \times \left[ 1 - \frac{I_{corr}}{I_{corr}^o} \right], \quad (1)$$

where  $I_{corr}^o$  and  $I_{corr}$  are the corrosion current densities of uninhibited and inhibited solutions, respectively.

TABLE 1: Polarisation parameters obtained for MS in 3.5% NaCl in the presence of various concentrations of Pec-g-PAAm.

S. no.	Conc. (ppm)	$E_{corr}$ (mV)	$I_{corr}$ ( $\mu A$ )	IE (%)	$R_p$ (ohms)	IE (%)	$b_a$	$b_c$	Corrosion rate (mpy)
1	Blank	-586	48.44		636		97.8	608	22.070
2	300	-529	38.64	35	815	21.96	100	313	17.58
3	500	-626	26	56.275	1525	58.30	80	151	11.917
4	600	-382	27.253	54.167	2026	68.61	83	217	12.397
5	700	-412	15	74.774	1154	81.45	81	147	7
6	800	-437	15.76	73.496	1180	85.53	87	98	7.100
7	900	-438	12.006	79.809	1047	64.62	89	76	5

TABLE 2: Polarisation parameters obtained for MS in 3.5% NaCl in the presence of various concentrations of Pec-g-PAA.

S. no.	Conc. (ppm)	$E_{corr}$ (mV)	$I_{corr}$ ( $\mu A$ )	IE (%)	$R_p$ (ohms)	IE (%)	$b_a$	$b_c$	Corrosion rate (mpy)
1	Blank	-586.7	48.44		636		97.8	608	22.07
2	50	-669	27	44.26	1344	52.68	100	309	12.56
3	100	-748	7.88	83.73	2463	74.18	91	167	3.584
4	200	-792	7.325	84.87	2527	74.83	97	111	3.120
5	300	-786	7.189	85.15	2594	75.48	93	119	3.270
6	400	-691	14.3	70.47	2505	74.61	214	229	6.500
7	500	-880	13.39	52.31	2090	69.57	351	72	7

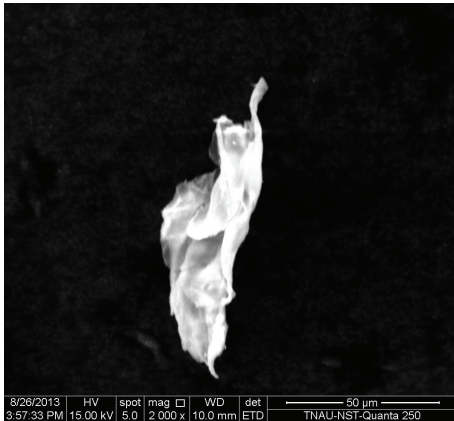


FIGURE 4: Scanning electron microscopic image of pectin.

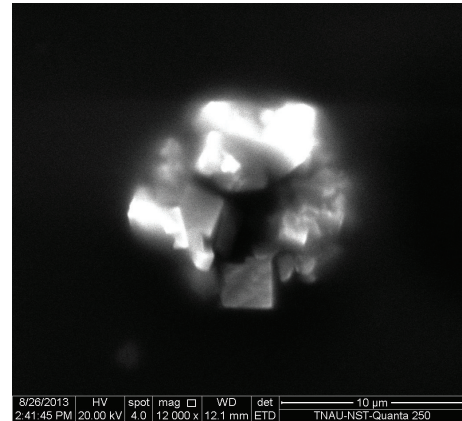


FIGURE 5: Scanning electron microscopic image of Pec-g-PAAm (magnified view).

The inhibition efficiency can be calculated using the polarization resistance ( $R_p$ ) using the formula

$$IE (\%) = \frac{R_p - R_p^0}{R_p} \times 100, \quad (2)$$

where  $R_p$  and  $R_p^0$  are the resistances of inhibited and uninhibited solutions, respectively.

### 3. Results and Discussion

#### 3.1. Characterisation

3.1.1. FTIR Spectrum Analysis. The FTIR spectrum of the pectin and Pec-g-PAAm and Pec-g-PAA are shown in

Figure 1. The possible structure of the grafted polymers and the scheme of synthesis are shown in Scheme 1 [10].

*Pec-g-PAAm*. The broad peaks in the range of  $3196$  to  $3322 \text{ cm}^{-1}$  are attributed to the overlapped  $-\text{OH}$  groups of pectin and symmetric and asymmetric  $-\text{NH}$  stretching vibrations of polyacrylamide. The peak at  $1655 \text{ cm}^{-1}$  accompanied by a shoulder peak at  $1610 \text{ cm}^{-1}$  is assigned to amide I and amide II bands, respectively, which confirms the formation of polyacrylamide. The small peak corresponding to  $1710 \text{ cm}^{-1}$  is an evidence for the presence of  $-\text{C}=\text{O}$  stretching of the polyacrylamide. The supporting evidence for the polyacrylamide grafted pectin is given by the  $-\text{CN}$  stretching peak

TABLE 3: Impedance parameters and inhibition efficiency values for mild steel sample in 3.5% NaCl containing various concentrations of Pec-g-PAAm.

S. no.	Conc. (ppm)	$R_s$ (ohms)	$R_p$ (ohms)	$R_{ads}$ (ohms)	Total resistance	IE (%)	$C_{ads}$ $10^{-4}$ F	$C_{dl}$ $10^{-3}$ F	Surface coverage ( $\theta$ )	$W$ ohms $s^{-1/2}$
1	Blank	2.018	56.25		58.3			3.72		
2	300	3.227	269	0.9797	273.2	78.7	3.42	2.30	0.38	122.6
3	500	3.552	294.1	4.853	302.5	80.7	5.47	0.388	0.89	94.15
4	600	3.692	317.9	13.19	334.8	82.6	0.321	0.206	0.94	128.9
5	700	3.102	548.4	12.03	563.5	89.7	0.210	0.182	0.95	101.7
6	800	3.727	491.7	25.32	520.7	88.8	0.666	0.175	0.95	91.69
7	900	3.569	195.4	17.47	216.4	73.1	0.977	0.460	0.87	98

TABLE 4: Impedance parameters and inhibition efficiency values for mild steel sample in 3.5% NaCl containing various concentrations of Pec-g-PAA.

S. no.	Conc. (ppm)	$R_s$ (ohms)	$R_p$ (ohms)	$R_{ads}$ (ohms)	Total resistance (ohms)	IE (%)	$C_{ads}$ $10^{-4}$ F	$C_{dl}$ $10^{-3}$ F	Surface coverage ( $\theta$ )	$W$ ohms $s^{-1/2}$
1	Blank	5.018	53.25		58.268			3.721		
2	50	6.026	179.4	2.31	187.73	69.0	66.84	0.7793	0.38	122
3	100	6.527	199.1	7.102	212.72	72.6	57.25	0.5582	0.90	194
4	200	6.125	214.2	9.534	229.85	74.7	12.31	0.4794	0.94	188
5	300	8.44	292	13.04	313.48	81.4	10.31	0.2040	0.95	202
6	400	3.125	292.6	43.87	339.59	82.8	8.52	0.1338	0.95	304
7	500	6.101	302	20.91	329.01	82.3	12.51	0.1000	0.88	192

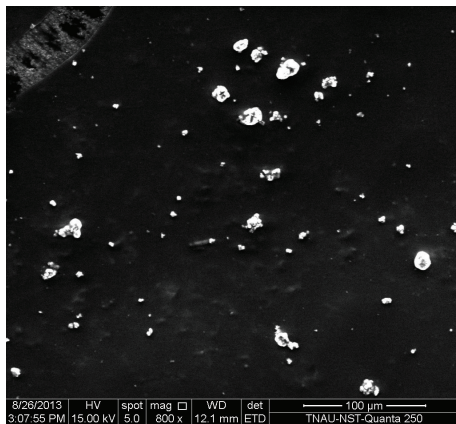


FIGURE 6: Scanning electron microscopic image of Pec-g-PAA.

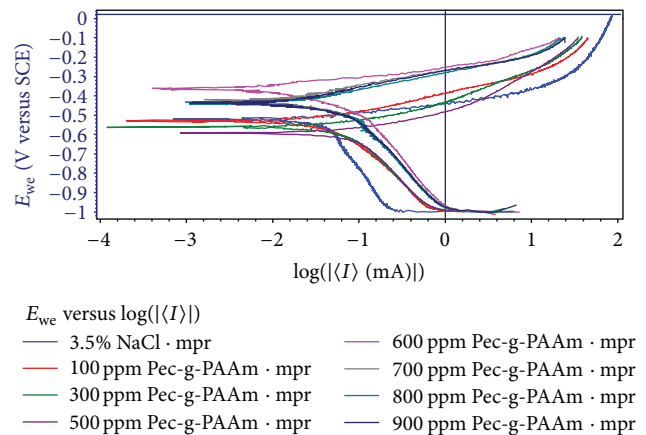


FIGURE 7

at  $1395\text{ cm}^{-1}$  and  $\text{C}-\text{O}$  stretching at  $1122\text{ cm}^{-1}$ . The peaks at  $1443\text{ cm}^{-1}$  and  $1353\text{ cm}^{-1}$  are attributed to the  $\text{CH}_2$  bending and  $\text{-CH}$  bending vibrations.

*Pec-g-PAA.* The broad peaks in the region of  $3200\text{--}2942\text{ cm}^{-1}$  are characteristic absorptions of  $\text{-OH}$  groups of pectin and polyacrylic acid. The polyacrylic acid grafted onto the pectin backbone is further confirmed by the presence of intense absorption of carbonyl group in the region of  $1709\text{ cm}^{-1}$ . The peak at  $1402\text{ cm}^{-1}$  corresponds to the symmetric stretching of the  $\text{COOH}$  anion groups. The  $\text{C}-\text{O}-\text{C}$  asymmetric stretching

and  $\text{C}-\text{O}$  stretching are confirmed with the absorption around  $1173\text{ cm}^{-1}$  and  $1003\text{ cm}^{-1}$  [14].

*3.1.2. Thermogravimetric Analysis.* Thermal degradation profiles of the grafted polymers were studied and the corresponding thermograms are presented in Figures 2 and 3. For Pec-g-PAAm, the thermal degradation occurs in three stages. The first step of degradation occurs in the range of  $30\text{--}200^\circ\text{C}$  where a weight loss of 14.6% is observed. This could be due to loss of entrapped water molecules and volatile impurities along with degradation of soft segment of Pec-g-PAAm [15]. The weight loss in this step may be assigned to the loss of

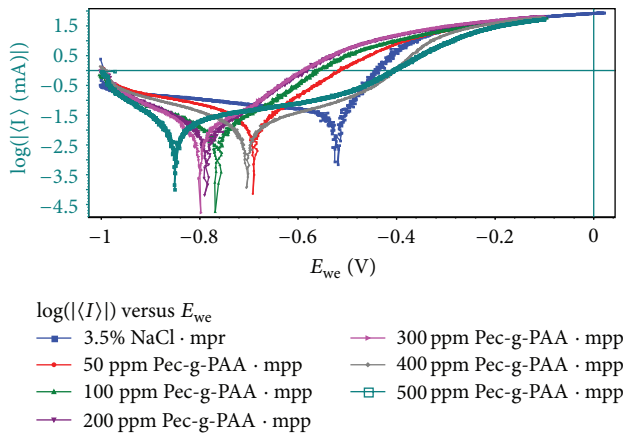


FIGURE 8

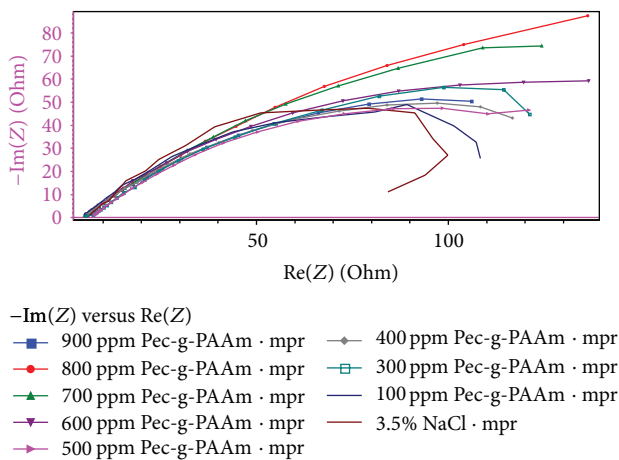


FIGURE 9

grafted links between the pectin and polyacrylamide. The second step of degradation occurs at 200–300°C, where a weight loss of 9.53% and 4.93% is observed indicating the loss of lateral chains of the polymer. The final step of degradation occurs in the range of 300–600°C with a major weight loss indicating the breakdown of the polymer backbone matrix [16].

A similar trend was observed for Pec-g-PAA till 200°C. But the second step of degradation occurs steadily compared to that in Pec-g-PAAm which is attributed to the easy breaking up of the lateral chains of the polymer. At 350°C there is a steep fall, indicating major mass loss at this temperature. In the temperature range of 350–600°C, further breakdown of the polymer backbone matrix might have taken place.

This thermal degradation profile provides an additional evidence for the grafting of the polymers and also ensures the use of the polymers even at high temperature saline environments.

**3.1.3. Scanning Electron Microscopic Analysis.** The microstructure morphology of the pectin, Pec-g-PAAm and Pec-g-PAA is shown in the Figures 4–6, respectively. In Figures 5 and 6, the distribution of grafted polymeric particles can be

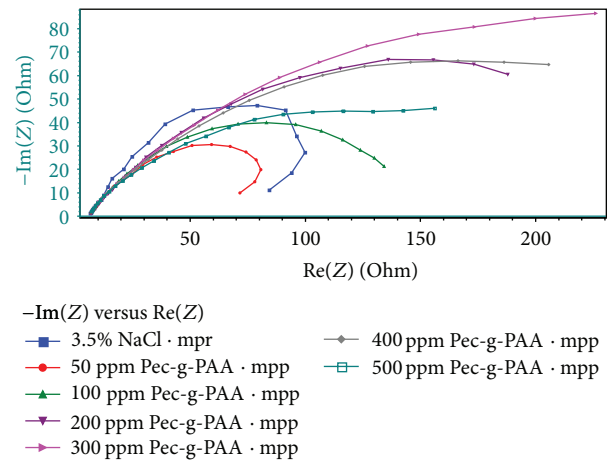


FIGURE 10

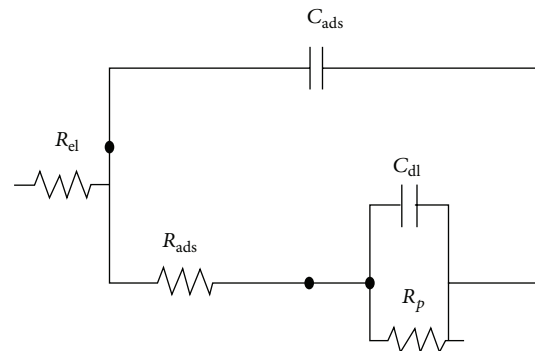


FIGURE 11: Equivalent circuit model used to fit the impedance data.

observed. Pectin is specifically called pectinic acid which is a polyacid. The interaction of pectinic acid and acrylamide depends on ionization of the polyacid and structural compatibility between the polymers [17]. When pectin gets dissolved in water, it exists as complex network-like structures containing branched and linear structures in the form of rods, segmented rods, and kinked rods [18, 19]. In this case, pectin appears like a feather-like structure (Figure 4). In Figures 5 and 6, a floral structure composed of agglomerated feather-like portion containing crystalline particles can be found which accounts for the grafted structure of the polymer. Such an organization potentially reveals the grafted structure of the polymers on the pectin scaffold.

### 3.2. Electrochemical Studies

**3.2.1. Tafel Extrapolation.** The polarization parameters calculated for the pectin grafted polymers are listed in Tables 1 and 2. The polarisation curves for the pectin grafted polymers are shown in Figures 7 and 8.

**Pec-g-PAAm.** The potentiodynamic anodic and cathodic polarisation curves of mild steel in NaCl medium containing different concentrations of the grafted polyacrylamide are presented in Figure 7 and the corresponding electrochemical

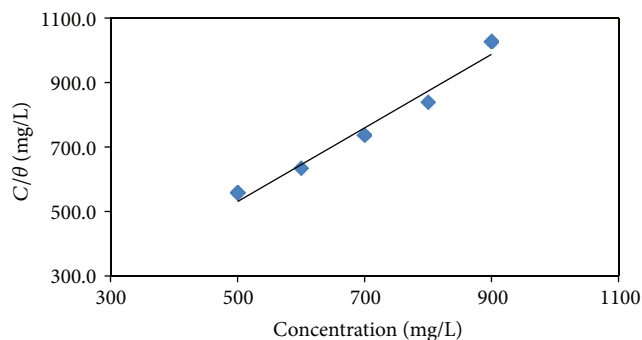


FIGURE 12: Langmuir isotherm for adsorption of Pec-g-PAAm on mild steel in NaCl.

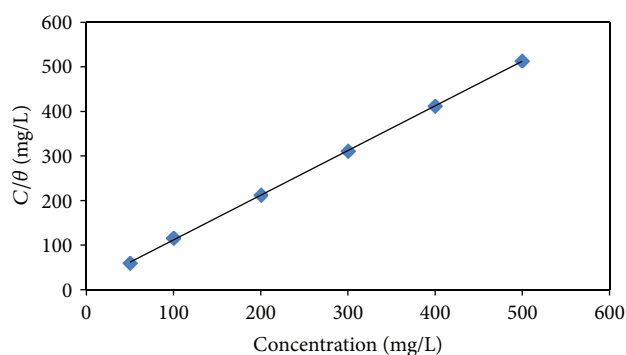


FIGURE 13: Langmuir isotherm for adsorption of Pec-g-PAA on mild steel in NaCl.

parameters are listed in Table 1. The data clearly shows that the  $E_{\text{corr}}$  values shift to more positive values, and corrosion current density is reduced. Ferreira et al. [20] have reported that (i) if the displacement in ( $E_{\text{corr}}$ ) values is  $>85$  mV *in inhibited system with respect to uninhibited, the inhibitor could be recognized as cathodic or anodic type and (ii) if displacement in  $E_{\text{corr}}$  is  $<85$  mV, it could be recognized as mixed-type*. In this case, the shift in  $E_{\text{corr}}$  values is more than 85 mV, and analysis of the polarisation curves shows that the anodic current density is reduced significantly compared to the cathodic current density. Hence the polymer under investigation must be predominantly an anodic inhibitor inhibiting the anodic dissolution reaction [21, 22].

**Pec-g-PAA.** Inspection of the polarisation curves (Figure 8) of Pec-g-PAA reveals that the cathodic current density is controlled to a greater extent compared to the anodic current density. Though oxygen is present in the solution, the decrease in the cathodic current density cannot be attributed to the oxygen reduction, because oxygen reduction might have reached a diffusion-controlled limit which is not observed in the polarisation plot [23]. Thus we can conclude that the grafted polyacrylic acid controls the corrosion process mainly by blocking the cathodic sites rather than the anodic sites, and the polymer is a moderate cathodic inhibitor and not of much anodic inhibitor [24]. The shape of the polarisation curves remains the same which indicates

that the cathodic and anodic reactions are not much altered throughout the corrosion process.

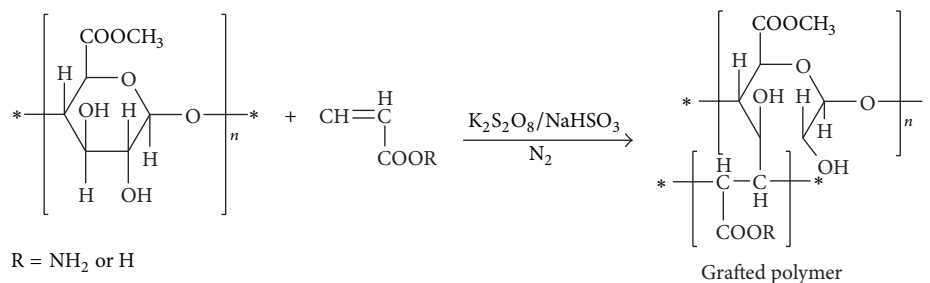
Non-Tafel behaviour is observed for NaCl medium and several authors have reported that accurate Tafel extrapolation is impossible due to nonlinearity of the Tafel region. Amin et al. [25] explained that the disparity in the anodic branch is due to nonpassive surface film formed by the deposition of the corrosion products, but with respect to the cathodic branch, diffusion of oxidizing species will be slow since the solution is stagnant and concentration polarization can act to shorten the cathodic linear Tafel region. In extreme cases, linearity may disappear completely, with the cathodic reaction now under combined activation and diffusion controlled at the corrosion potential ( $E_{\text{corr}}$ ). Due to the above reasons accurate evaluation of Tafel slopes is not possible.

However, in this report, a reasonable fit is achieved with the cathodic data, and the extrapolation of the cathodic Tafel lines to the corrosion potential yields reasonable values of corrosion current density,  $I_{\text{corr}}$ , and that presented in Table 2 [26].

The results listed in the table reveal that there is a decrease in corrosion current density with increase in polarisation resistance and inhibition efficiency, which is in well accordance with the dependency on inhibitor concentration. A definite negative shift in the  $E_{\text{corr}}$  values suggests that the inhibitor is a strong cathodic inhibitor as it dominantly controls the cathodic reduction reaction [27].

**3.2.2. Impedance Circles.** The Nyquist plots in the presence and absence of various concentrations of Pec-g-PAAm and Pec-g-PAA are given in Figures 9 and 10, respectively. The Nyquist plots are single capacitive semicircles which show that the corrosion process is governed by charge-transfer process [28]. The diameters of the semicircles increase with the increasing inhibitor concentration. The impedance spectrum for mild steel in neutral media is interpreted with two time constants by using a simple equivalent circuit which represents an imperfectly covered electrode [29–31].

The equivalent circuit proposed to fit the impedance data of both the grafted polymers is shown in Figure 11. The  $R_{\text{ads}}/C_{\text{ads}}$  is the high frequency time constant attributed to the adsorption of the inhibitor and  $R_p/C_{\text{dl}}$  is the low frequency time constant attributed to the defect sites where charge transfer processes take place. Different parameters obtained from the fit are listed in Tables 3 and 4 and analysed. The total resistance of the system is calculated by adding all the resistances  $R_{\text{el}}$ ,  $R_{\text{ads}}$ , and  $R_p$  [32] and the corresponding inhibition efficiency obtained is given in the table. From the table, it is evident that the resistance values increased and the capacitance values decreased. The decrease in capacitance values is due to the adsorption of the inhibitor molecules on the surface thereby causing a change in the double layer. The double layer in between the charged metal surface and solution is considered as electrical capacitor. Therefore, the adsorption of the inhibitor on the metal surface decreases the electrical capacitance of the metal and also displaces the water molecules and other ions adsorbed on the surface and forms a protective layer [33, 34].



SCHEME 1: Synthesis route to Pec-g-PAAm and Pec-g-PAA.

#### 4. Adsorption Considerations

The information about the interaction between the inhibitor molecules and the mild steel can be provided by fitting the surface coverage data obtained from the double layer capacitance ( $C_{dl}$ ) values of impedance spectroscopy using the following formula:

$$\text{Surface coverage } (\theta) = \left[ \frac{C_{dl}^{\circ} - C_{dl}}{C_{dl}^{\circ}} \right], \quad (3)$$

where  $C_{dl}^{\circ}$  and  $C_{dl}$  are the double-layer capacitance values without and with the inhibitor. A plot of  $C/\theta$  versus  $C$  (Figures 12 and 13) gave straight lines with linear regression coefficient values very close to unity, which indicates that the adsorption of inhibitor molecules on the mild steel surface obeys Langmuir isotherm model.

#### 5. Conclusion

Grafting of polyacrylamide and polyacrylic acid onto the backbone of pectin was achieved and a water soluble polymer product was obtained. Since pectin is a natural polymer extensively used in drug delivery applications, grafting of heteroatoms-containing monomers like acrylamide and acrylic acid makes them suitable for use as environmentally benign corrosion inhibitors. The grafting certainly improved the inhibition efficiency when compared to the homopolymers, namely, polyacrylamide and polyacrylic acid [26, 35]. The obtained water soluble polymers when tested for the corrosion performance on mild steel in neutral medium by electrochemical methods provided appreciable results. The graft polymer containing polyacrylamide provided slightly higher corrosion inhibition efficiency than that of polyacrylic acid-containing polymer. This could be attributed to the nitrogen heteroatom present in the polyacrylamide.

#### Conflict of Interests

The authors declare that there is no conflict of interests regarding the publication of this paper.

#### References

- [1] H. F. Mark, N. G. Gaylord, and N. M. Bikales, "Encyclopaedia of polymer science and technology," in *Amorphous Polymers*, vol. 1, p. 558, John Wiley & Sons, 2nd edition, 1964.
- [2] M. A. Amin, S. S. A. El-Rehim, E. E. F. El-Sherbini, O. A. Hazzazi, and M. N. Abbas, "Polyacrylic acid as a corrosion inhibitor for aluminium in weakly alkaline solutions. Part I: weight loss, polarization, impedance EFM and EDX studies," *Corrosion Science*, vol. 51, no. 3, pp. 658–667, 2009.
- [3] D. E. Arthur, A. Jonathan, P. O. Ameh, and C. Anya, "A review on the assessment of polymeric materials used as corrosion inhibitor of metals and alloys," *International Journal of Industrial Chemistry*, vol. 4, no. 1, 2013.
- [4] Y. Xu, L. Zhao, L. Wang, S. Xu, and Y. Cui, "Synthesis of polyaspartic acid-melamine grafted copolymer and evaluation of its scale inhibition performance and dispersion capacity for ferric oxide," *Desalination*, vol. 286, pp. 285–289, 2012.
- [5] Y. Ren, Y. Luo, K. Zhang, G. Zhu, and X. Tan, "Lignin terpolymer for corrosion inhibition of mild steel in 10% hydrochloric acid medium," *Corrosion Science*, vol. 50, no. 11, pp. 3147–3153, 2008.
- [6] M. M. Fares, A. K. Maayta, and M. M. Al-Qudah, "Pectin as promising green corrosion inhibitor of aluminum in hydrochloric acid solution," *Corrosion Science*, vol. 60, pp. 112–117, 2012.
- [7] S. Banerjee, V. Srivastava, and M. M. Singh, "Chemically modified natural polysaccharide as green corrosion inhibitor for mild steel in acidic medium," *Corrosion Science*, vol. 59, pp. 35–41, 2012.
- [8] E. Akbarzadeh, M. N. M. Ibrahim, and A. A. Rahim, "Corrosion inhibition of mild steel in near neutral solution by Kraft and Soda lignins extracted from oil palm empty fruit bunch," *International Journal of Electrochemical Science*, vol. 6, no. 11, pp. 5396–5416, 2011.
- [9] R. K. Mishra, A. K. Banthia, and A. B. A. Majeed, "Pectin based formulations for biomedical applications: a review," *Asian Journal of Pharmaceutical and Clinical Research*, vol. 5, pp. 1–7, 2012.
- [10] R. K. Mishra, P. B. Sutar, J. P. Singhal, and A. K. Banthia, "Graft copolymerization of pectin with polyacrylamide," *Polymer*, vol. 46, no. 11, pp. 1079–1085, 2007.
- [11] P. B. Sutar, R. K. Mishra, K. Pal, and A. K. Banthia, "Development of pH sensitive polyacrylamide grafted pectin hydrogel for controlled drug delivery system," *Journal of Materials Science*, vol. 19, no. 6, pp. 2247–2253, 2008.
- [12] N. M. Ranjha, J. Mudassir, and Z. Z. Sheikh, "Synthesis and characterization of pH-Sensitive pectin/Acrylic acid hydrogels for verapamil release study," *Iranian Polymer Journal*, vol. 20, no. 2, pp. 147–159, 2011.
- [13] S. Rajendran, B. V. Apparao, and N. Palaniswamy, "Synergistic and antagonistic effects existing among polyacrylamide, phenyl phosphonate and Zn<sup>2+</sup> on the inhibition of corrosion of mild

- steel in a neutral aqueous environment," *Electrochimica Acta*, vol. 44, no. 2-3, pp. 533-537, 1998.
- [14] M. F. Rosa, E. S. Medeiros, J. A. Malmonge et al., "Cellulose nanowhiskers from coconut husk fibers: effect of preparation conditions on their thermal and morphological behavior," *Carbohydrate Polymers*, vol. 81, no. 1, pp. 83-92, 2010.
- [15] M. Zendejdel, A. Barati, and H. Alikahani, "Preparation and characterization of poly(acryl amide-coacrylic acid)/nan and Clinoptilolite nanocomposites with improved methylene blue dye removal behavior from aqueous solution," *E-Polymers*, vol. 2, no. 1, 2011.
- [16] H. Bhandari, V. Choudhary, and S. K. Dhawan, "Synergistic effect of copolymers composition on the electrochemical, thermal, and electrical behavior of 5-lithiosulphoisophthalic acid doped poly(aniline-co-2-isopropylaniline): synthesis, characterization, and applications," *Polymers for Advanced Technologies*, vol. 20, no. 12, pp. 1024-1034, 2009.
- [17] L. Liu, P. H. Cooke, D. R. Coffin, M. L. Fishman, and K. B. Hicks, "Pectin and polyacrylamide composite hydrogels: effect of pectin on structural and dynamic mechanical properties," *Journal of Applied Polymer Science*, vol. 92, no. 3, pp. 1893-1901, 2004.
- [18] M. L. Fishman, P. Cooke, A. Hotchkiss, and W. Damert, "Progressive dissociation of pectin," *Carbohydrate Research*, vol. 248, pp. 303-316, 1993.
- [19] M. L. Fishman, H. K. Chau, P. Hoagland, and K. Ayyad, "Characterization of pectin, flash-extracted from orange albedo by microwave heating, under pressure," *Carbohydrate Research*, vol. 323, no. 1-4, pp. 126-138, 2000.
- [20] E. S. Ferreira, C. Giancomelli, F. C. Giacomelli, and A. Spinelli, "Evaluation of the inhibitor effect of l-ascorbic acid on the corrosion of mild steel," *Materials Chemistry and Physics*, vol. 83, no. 1, pp. 129-134, 2004.
- [21] W. H. Li, Q. He, C. L. Pei, and B. R. Hou, "Some new triazole derivatives as inhibitors for mild steel corrosion in acidic medium," *Journal of Applied Electrochemistry*, vol. 38, no. 3, pp. 289-295, 2008.
- [22] M. K. Pavithra, T. V. Venkatesha, K. Vathsala, and K. O. Nayana, "Synergistic effect of halide ions on improving corrosion inhibition behaviour of benzoisothiazole-3-piperazine hydrochloride on mild steel in 0.5 M H<sub>2</sub>SO<sub>4</sub> medium," *Corrosion Science*, vol. 52, no. 11, pp. 3811-3819, 2010.
- [23] S. A. Umoren, Y. Li, and F. H. Wang, "Synergistic effect of iodide ion and polyacrylic acid on corrosion inhibition of iron in H<sub>2</sub>SO<sub>4</sub> investigated by electrochemical techniques," *Corrosion Science*, vol. 52, no. 7, pp. 2422-2429, 2010.
- [24] L. Feng, H. Yang, and F. Wang, "Experimental and theoretical studies for corrosion inhibition of carbon steel by imidazoline derivative in 5% NaCl saturated Ca(OH)<sub>2</sub> solution," *Electrochimica Acta*, vol. 58, pp. 427-436, 2011.
- [25] M. A. Amin, S. S. A. El-Rehim, E. E. F. El-Sherbini, O. A. Hazzazi, and M. N. Abbas, "Polyacrylic acid as a corrosion inhibitor for aluminium in weakly alkaline solutions. Part I: weight loss, polarization, impedance EFM and EDX studies," *Corrosion Science*, vol. 51, no. 3, pp. 658-667, 2009.
- [26] S. A. Umoren, Y. Li, and F. H. Wang, "Synergistic effect of iodide ion and polyacrylic acid on corrosion inhibition of iron in H<sub>2</sub>SO<sub>4</sub> investigated by electrochemical techniques," *Corrosion Science*, vol. 52, no. 7, pp. 2422-2429, 2010.
- [27] F. Bentiss, M. Traisnel, and M. Lagrenee, "The substituted 1,3,4-oxadiazoles: a new class of corrosion inhibitors of mild steel in acidic media," *Corrosion Science*, vol. 42, no. 1, pp. 127-146, 2000.
- [28] R. Rosliza, H. B. Senin, and W. B. W. Nik, "Electrochemical properties and corrosion inhibition of AA6061 in tropical seawater," *Colloids and Surfaces A*, vol. 312, no. 2-3, pp. 185-189, 2008.
- [29] H. H. Uhlig and R. W. Revie, *Uhlig's Corrosion Handbook*, vol. 1207, John Wiley Sons, 2000.
- [30] U. Rammelt, S. Koehler, and G. Reinhard, "Use of vapour phase corrosion inhibitors in packages for protecting mild steel against corrosion," *Corrosion Science*, vol. 51, no. 4, pp. 921-925, 2009.
- [31] U. Rammelt, S. Koehler, and G. Reinhard, "Electrochemical characterisation of the ability of dicarboxylic acid salts to the corrosion inhibition of mild steel in aqueous solutions," *Corrosion Science*, vol. 53, no. 11, pp. 3515-3520, 2011.
- [32] M. Vakili Azghandi, A. Davoodi, G. A. Farzi, and A. Kosari, "Water-base acrylic terpolymer as a corrosion inhibitor for SAE1018 in simulated sour petroleum solution in stagnant and hydrodynamic conditions," *Corrosion Science*, vol. 64, pp. 44-54, 2012.
- [33] M. Mahdavian and R. Naderi, "Corrosion inhibition of mild steel in sodium chloride solution by some zinc complexes," *Corrosion Science*, vol. 53, no. 4, pp. 1194-1200, 2011.
- [34] M. Lagrenee, B. Mernari, M. Bouanis, M. Traisnel, and F. Bentiss, "Study of the mechanism and inhibiting efficiency of 3,5-bis(4-methylthiophenyl)-4H-1,2,4-triazole on mild steel corrosion in acidic media," *Corrosion Science*, vol. 44, no. 3, pp. 573-588, 2002.
- [35] D. Chamovska, M. Cvetkovska, and T. Grchev, "Corrosion inhibition of iron in hydrochloric acid by polyacrylamide," *Journal of the Serbian Chemical Society*, vol. 72, no. 7, pp. 687-698, 2007.



**Hindawi**

Submit your manuscripts at  
<http://www.hindawi.com>

